1-1-2019

Alterations to the microbiota-colon-brain axis in high-fat-diet-induced obese mice compared to diet-resistant mice

Peng Zhang
Xuzhou Medical University, Jiangsu Key Laboratory of Immunity and Metabolism, University of Wollongong, zhangp@uow.edu.au

Yinghua Yu
Xuzhou Medical University, University of Wollongong, yinghua@uow.edu.au

Yanfang Qin
Xuzhou Medical University, Jiangsu Key Laboratory of Immunity and Metabolism

Yuan Zhou
Jiangsu Key Laboratory of Immunity and Metabolism, Xuzhou Medical University

Renxian Tang
Jiangsu Key Laboratory of Immunity and Metabolism, Xuzhou Medical University

See next page for additional authors

Alterations to the microbiota-colon-brain axis in high-fat-diet-induced obese mice compared to diet-resistant mice

Abstract

Obesity is underpinned by both genetic and environmental factors, including a high-saturated-fat diet. Some mice develop diet-induced obesity (DIO), but others remain diet resistant (DR) despite intake of the same high-saturated-fat diet, a phenomenon that mimics characteristics of the human obese phenotype. Microbiota-colon-brain axis regulation is important for energy metabolism and cognition. Using DIO and DR mouse models, this study aimed to examine gut microbiota, colonic inflammation and cognitive function to elucidate the role of microbiota-gut-brain regulation in DIO. C57Bl6/J mice fed a chronic saturated-palmitic-acid diet for 22 weeks showed significant body weight gain differences, with the top one third gaining 48% heavier body weight than the lower one third. There was significant reduction in gut microbiota richness and diversity in DIO mice but not in DR mice. At the phylum level, DIO mice had increased abundance of Firmicutes and Antinobacteria, and decreased abundance of Bacterioides and Proteobacteria in gut microbiota. DIO mice exhibited reduced tight junction proteins, increased plasma endotoxin lipopolysaccharide (LPS) and increased inflammation in the colon and liver. Recognition memory and spatial memory were impaired in DIO mice, associated with decreased Bacteroidetes. Further examination showed that hippocampal brain-derived neurotrophic factor was significantly decreased in DIO mice (vs. DR). Conversely, DR mice showed no changes in the above parameters measured. Therefore, gut microbiota, colon inflammation and circulating LPS may play a major role in the development of the obese phenotype and cognitive decline associated with a chronic high-saturated-palmitic-acid diet.

Disciplines

Medicine and Health Sciences

Publication Details

Zhang, P., Yu, Y., Qin, Y., Zhou, Y., Tang, R., Wang, Q., Li, X., Wang, H., Weston-Green, K., Huang, X. & Zheng, K. (2019). Alterations to the microbiota-colon-brain axis in high-fat-diet-induced obese mice compared to diet-resistant mice. Journal of Nutritional Biochemistry, 65 54-65.

Authors

Peng Zhang, Yinghua Yu, Yanfang Qin, Yuan Zhou, Renxian Tang, Qingling Wang, Xiangyang Li, Hongqin Wang, Katrina Weston-Green, Xu-Feng Huang, and Kuiyang Zheng

Alterations to the microbiota-colon-brain axis in high-fat diet-induced obese mice compared to diet-resistant mice

Peng Zhang[a,b,1], Yinghua Yu[a,b,1], Yanfang Qin[a], Yuan Zhou[a], Renxian Tang[a], Qingling Wang[a], Xiangyang Li[a], Hongqin Wang[b], Katrina Weston-Green[b], Xu-Feng Huang[a,b,*], Kuiyang Zheng[a,*]

Affiliation:

[a]Department of Pathogen Biology and Immunology, Xuzhou Medical University and Jiangsu Key Laboratory of Immunity and Metabolism, Xuzhou, Jiangsu 221004, China

[b]School of Medicine, University of Wollongong and Illawarra Health and Medical Research Institute (IHMRI), Wollongong, NSW 2522, Australia

[1] contributed equally to this paper

***Correspondence:**

Professor Kuiyang Zheng, MD, PhD, Department of Pathogen Biology and Immunology, Xuzhou Medical University and Jiangsu Key Laboratory of Immunity and Metabolism, Xuzhou, Jiangsu 221004, China. **E-mail:** zky02@163.com, **Tel.:** 86-516-83372002

Senior Professor Xu-Feng Huang, MD, PhD, MSc, Illawarra Health and Medical Research Institute and School of Medicine, University of Wollongong, Northfields Avenue, Wollongong, NSW 2522, Australia. **E-mail:** xhuang@uow.edu.au, **Tel:** 61-2- 4221 4300, ORCID: 0000-0002-5895-2253

A running title:

Microbiota-colon-brain axis in obese mice

Grants, sponsors, and funding sources:

This study was supported by Diabetes Australia Research Trust Research Project (Y12G-YUYI); The Priority Academic Program Development of Jiangsu Higher Education Institutions (PAPD); Dean Special Foundation of Xuzhou Medical University (2012KJZ07); General Financial Grant from the Chinese Postdoctoral Science Foundation (2014M561713); and The Program for Youth Science and Technology Innovative Research Team of Xuzhou Medical University.

Keywords:

palmitic acid diet, obesity, gut microbiota, colonic inflammation, cognition, BDNF

Abstract:

Obesity is underpinned by both genetic and environmental factors, including a high saturated fat diet. Some mice develop diet-induced obesity (DIO) but others remain diet-resistant (DR), despite intake of the same high-saturated fat diet; a phenomenon that mimics characteristics of the human obese phenotype. Microbiota-colon-brain axis regulation is important for energy metabolism and cognition. Using DIO and DR mouse models, this study aimed to examine gut microbiota, colonic inflammation and cognitive function to elucidate the role of microbiota-gut-brain regulation in diet-induced obesity. C57Bl6/J mice fed a chronic saturated palmitic acid diet for 22 weeks showed significant body weight gain differences, with the top one third gaining 48% heavier body weight than the lower one third. There was significant reduction in gut microbiota richness and diversity in DIO mice, but not in DR mice. At the phylum level, DIO mice had increased abundance of Firmicutes and Antinobacteria, and decreased abundance of Bacterioides and Proteobacteria in gut microbiota. DIO mice exhibited reduced tight junction proteins, increased plasma endotoxin lipopolysaccharide (LPS) and increased inflammation in the colon and liver. Recognition memory and spatial memory were impaired in DIO mice, associated with decreased Bacteroidetes. Further examination showed that hippocampal brain-derived neurotrophic factor (BDNF) was significantly decreased in DIO mice (vs DR). Conversely, DR mice showed no changes in the above parameters measured. Therefore, gut microbiota, colon inflammation and circulating LPS may play a major

role in the development of the obese phenotype and cognitive decline associated with a chronic high saturated palmitic acid diet.

Keywords:

palmitic acid diet, obesity, gut microbiota, colonic inflammation, cognition, BDNF

1 INTRODUCTION:

Diets rich in saturated fat can induce obesity, associated with insulin resistance and cognitive decline. Palmitic acid (PA, C16:0) is the most common saturated fatty acid in human diets in the modern society, accounting for approximately 65% of saturated fatty acids and 32% of total fatty acids in human serum [1]. Patients with metabolic syndrome have a significantly higher level of PA, but not other saturated fatty acids, such as myristic acid or stearic acid within erythrocytes [2]. Obesity is a polygenic disorder and results from a complex interaction with an obesogenic environment, including saturated fat intake [3]. For example, mice or rats fed a high-fat diet either develop obesity or resistance to obesity, but have comparable body weight when fed a lab chow diet [4-7]. Interestingly, there are differences in gene expression between diet-induced obesity (DIO) mice and their diet-resistant (DR) counterparts [8, 9], showing clear genetic distinction between resistant and non-resistant rodents. Therefore, DIO and DR models mimic some characteristics of the human obese phenotype, including a polygenic mode of inheritance and the fact that some (but not all) individuals are susceptible to weight gain when exposed to an obesogenic environment [10].

The role of gut microbiota in contributing to obesity has been recognized. For example, an imbalance of Firmicutes and Bacteroidetes, the primary bacterial phyla comprising the gastrointestinal microbiota, has been reported in the leptin-deficient ob/ob mouse model [10, 11]. Consistent with animal studies, similar differences with an increase in the ratio of Firmicutes/Bacteroidetes has been found in the distal gut

microbiota in obese individuals [12]. However, alterations in the gut microbiota in obese individuals have not been reported by all investigators [13]. It has even been reported that ratios of Firmicutes to Bacteroidetes are lower in some obese adults compared to lean controls [14], whereas a study employing an 8-week high-saturated fat diet altered gut microbiota with increased Firmicutes and reduced Bacteriodetes in mice [15]. However, rare studies have examined microbiota in obesity in a manner that encompasses the interaction between environmental and genetic factors using DIO compared to DR phenotypes.

Obesity has been associated with a chronic low-grade level of inflammation. Alterations in the gut microbiota may play a role in intestinal inflammation and epithelial functions in the development of obesity. High-fat dietary intake increases circulating plasma levels of lipopolysaccharide (LPS, endotoxin), a breakdown product of outer layer of Gram-negative bacteria [16]. LPS and saturated fatty acids exert effects on the toll-like receptor 4 (TLR4) [17], which is expressed at high levels in the colon, but lower levels in the small intestine [18, 19]. TLR4 and its adaptor protein, myeloid differentiation primary-response protein 88 (MyD88), activate the inflammatory signaling pathway, including inhibitor kappa B alpha (IκBα) and nuclear factor-kappa B (NFκB) [20]. In addition, intestinal macrophages are essential for intestinal homeostasis and play critical roles in protective immunity and inflammation [21, 22]. The colon has a high density of macrophages compared to other parts of the gastrointestinal tract [23]. In the healthy mouse colon, most resident macrophages are resistant to TLR stimulation and express anti-inflammatory markers,

such as CD206, to prevent inflammation [24]. On the other hand, experimental colitis results in the accumulation of TLR-responsive pro-inflammatory macrophages, most of which become CD11c+ and F4/80+, indicating upregulated pro-inflammatory actions [24]. A recent report showed that colonic pro-inflammatory macrophages play a causal role in the development of insulin resistance, as decreased infiltration of colonic pro-inflammatory macrophages improved high-fat diet-induced insulin resistance in macrophage-specific chemokine (C-CMotif) receptor 2 (Ccr2) knockout (M-Ccr2KO) mice [25]. Another study found that the switch from anti-inflammatory to pro-inflammatory macrophages occurred in adipose and muscle tissue, as well as the liver and pancreas, contributing to insulin resistance in obesity [26]. However, the status of macrophages in the colon of DIO and DR mice requires further investigation. Furthermore, the role of colonic inflammation in generating obesity induced by a high saturated fat diet and altered gut microbiota is unknown.

Evidence shows a link between gut microbiota, central levels of brain-derived neurotrophic factor (BDNF) and cognitive behavior. For example, one study showed that administration of gut bacteria *Citrobacter rodentium* by oral gavage caused memory dysfunction in mice exposed to stress conditions [27], while another reported that oral antimicrobial treatment transiently altered the composition of the microbiota and increased hippocampal BDNF expression [28]. On the other hand, reduced BDNF expression in the hippocampus contributes to working-memory impairment in germ-free mice [27]. These studies suggest that BDNF may be influenced by gut microbiota, causing effects on cognitive function. However, it is not

known whether cognition and altered BDNF levels are affected by a diet high in saturated palmitic acid or by the presence of obesity, and whether alterations in these factors occur concurrently with altered gut microbiota.

A useful tool in preclinical obesity research to study the interaction between diet and genes is the C57 male mouse model, incorporating mice genetically prone to diet-induced obesity and their diet-resistant counterparts. When exposed to a high-fat diet, the DIO mice gain weight and become obese, while the DR mice remain as lean as the control mice. Therefore, the DIO and DR mouse model can provide insight into whether changes in the gut microbiota, colon inflammation and cognition are driven by the high saturated PA diet or by the ensuing obesity. In the current study, by using both chow- and PA diet-fed DIO and DR mice, we determined whether shifts in the microbiota profile result solely from the consumption of an obesogenic PA diet or are a manifestation of the obese phenotype. Furthermore, we examined levels of LPS (an endotoxin) in plasma, colonic tight junction protein levels (reflecting the permeability of colon epithelia), macrophage shifting towards a pro-inflammatory phenotype and markers of inflammation in the colon, as well as hippocampal BDNF and cognitive behavior.

2 MATERIALS AND METHODS:

2.1 Animals and treatments

Seventy-two C57Bl/6J male mice (6 weeks old) were obtained from the Animal Resources Center (Perth, WA, Australia). They were housed in environmentally

controlled conditions (temperature 22°C, 12 hour light/dark cycle), and allowed ad libitum access to food and water through-out the study. Mice were fed standard laboratory chow (ie low fat (LF) diet, AIN93M, Speciality Feeds, WA, Australia) for the first week to facilitate habituation to the new environment, then randomized into dietary treatment groups. The first group of mice (n=18) was fed a LF diet as a control, while the second group (n=54) was fed a high PA diet for 22 weeks. High PA diets were custom-made by Specialty Feeds (SF15-080, WA Australia) and contained 300 g/kg as fat (30%), including 100 g/kg palmitate (ie palmitate equivalent to 30% of total fat composition). The rationale for choosing this lipid composition was based on the average saturated fat content of a hamburger (ie a typical modern Western human fast food meal item), which can be more than 30%. The LF diet was used as a control, with a crude fat content of 4% (PA, 0.008%). After consuming the high PA diet for 8-weeks, the mice with the highest body weight gain were designated as the DIO mice (n=18), while mice with the lowest body weight gain were designated as the DR mice (n=18), according to methods we have previously published [29, 30] Mice with an intermediate body weight gain were removed from this study.

After 19 weeks of consuming either a high PA or LF diet, mice underwent an intraperitoneal glucose tolerance test (IPGTT, Section 2.2 below), followed by a series of behavioural tests in weeks 20-21 (Section 2.3). Mice were sacrificed after 22-weeks of dietary treatment, 4 days after behavioural testing. Four fat pads (Inguinal, Epididymal, Perirenal, Mesenteric) were excised and weighed. Each group of mice (n=18) were further divided into 3 subgroups (n=6) for tissue examination:

immunohistochemistry in colon and liver after fixing tissue; Western blot in colon and liver; In situ in brain and microbial diversity analysis in cecal content. Samples of plasma, intestine and cecal content, as well as liver and brain tissues were collected and stored at -80 °C for further analyses. All experimental procedures were approved by the Animal Ethics Committee, University of Wollongong, Australia, and all animal experiments were conducted in compliance with National Health and Medical Research Council (NHMRC) *Australian Code of Practice for the Care and Use of Animal for Scientific Purposes (2004).*

2.2 Intraperitoneal glucose tolerance test (IPGTT)

The IPGTT was conducted as we have previously described [31]. Briefly mice were fasted overnight followed by an intraperitoneal injection of glucose (0.5 g/kg; Sigma-Aldrich, St Louis, MO, USA). Blood samples were obtained from the tail vein at 0, 30, 60 and 120 minutes following the injection of glucose. Blood glucose levels were measured in duplicate using an Accu-Chek glucometer (Roche Diagnostics GmbH Mannheim, Germany).

2.3 Behavioral tests

The Y-maze and novel object recognition tests were performed in order to examine dietary effects on spatial and recognition memory. Tests were conducted based on methods previously published [32, 33] (see Supporting Information for detailed methods). In the Y-maze test, the ratio of time spent in the novel arm (a

ratio of the amount of time spent in the novel arm over the total time spent in all three arms) was used to evaluate spatial memory. For the novel object recognition test, the discrimination index ([(Novel object exploration time/Total exploration time)−(Familiar object exploration time/Total exploration time)]×100) was used to evaluate recognition memory.

2.4 Plasma leptin and adiponectin

Post-mortem blood was collected directly from the heart into a heparin coated tube. Blood samples were centrifuged at 4000rpm for 10 minutes (4^{o}C) and plasma was collected. Using the mouse endocrine Lincoplex kit (Cat.# MENDO-75K, Linco Research, St Louis, MO, USA), the plasma levels of leptin and adiponectin were determined.

2.5 Haematoxylin and eosin (H & E) staining

Paraffin-embedded liver sections (5µm) were stained with hematoxylin and eosin. The histological parameters (steatosis and ballooning) were scored using a method described in our previous study [34] (see Supporting Information for detailed methods).

2.6. Immunohistochemistry

The immunohistochemical staining method for liver or colon sections was conducted using the protocol we have previously published [34] (see Supporting Information for detailed methods).

2.7 Western blotting

Colon tissues were dissected and homogenized in a NP-40 lysis buffer (containing NP40, Protease Inhibitor Cocktail, 1 mM PMSF and 0.5 mM β -glycerophosphate). Total protein concentrations were determined by DC-Assay (Bio-Rad, Hercules, CA) and detected using a SpectraMax Plus384 absorbance microplate reader (Molecular Devices, Sunnyvale, CA). The Western blot method was conducted as described in our previous study [35] (see Supporting Information for detailed methods).

2.8 Lipopolysaccharide (LPS) determination

The concentration of circulating plasma LPS was measured by enzyme-linked immunosorbent assay (LAL assay kit, Hycult Biotech, The Netherlands). The absorbance was measured at 405 nm using a spectrophotometer, with measurable concentrations ranging from 0.04 to 10 EU/ml. All samples for LPS measurements were performed in duplicate.

2.9 Microbial diversity analysis

2.9.1 DNA extraction and PCR amplification

Microbial DNA was extracted from cecal content using the E.Z.N.A.® stool DNA Kit (Omega Bio-tek, Norcross, GA, U.S.) according to manufacturer's protocols. The V4-V5 regions of the bacteria 16S ribosomal RNA gene were amplified by PCR (95 °C for 2 min, followed by 25 cycles at 95 °C for 30 s, 55 °C for 30 s, and 72 °C for 45 s with a final extension at 72 °C for 5 min) using primers 338F 5'-barcode-ACTCCTACGGGAGGCAGCAG)-3' and 806R 5'-GGACTACHVGGGTWTCTAAT-3', where the barcode was an eight-base sequence unique to each sample. PCR reactions were performed in triplicate with 20 μL mixture containing 4 μL of 5 × FastPfu Buffer, 2 μL of 2.5 mM dNTPs, 0.8 μL of each primer (5 μM), 0.4 μL of FastPfu Polymerase, and 10 ng of template DNA.

2.9.2 Illumina MiSeq sequencing

Amplicons were extracted from 2% agarose gels and purified using the AxyPrep DNA Gel Extraction Kit (Axygen Biosciences, Union City, CA, USA) according to the manufacturer's instructions and quantified using QuantiFluor™ -ST (Promega, U.S.). Purified amplicons were pooled in equimolar and paired-end sequenced (2 × 250) on an Illumina MiSeq platform according to standard protocols.

2.9.3 Processing of sequencing data

Raw fastq files were demultiplexed, quality-filtered using QIIME (version 1.17) with the following criteria: (i) The 300 bp reads were truncated at any site receiving an average quality score <20 over a 50 bp sliding window, discarding the truncated reads that were shorter than 50bp. (ii) exact barcode matching, 2 nucleotide mismatch

in primer matching, reads containing ambiguous characters were removed. (iii) only sequences that overlap longer than 10 bp were assembled according to their overlap sequence. Readings that could not be assembled were discarded.

Operational Units (OTUs) were clustered with 97% similarity cut-off using UPARSE (version 7.1 http://drive5.com/uparse/) and chimeric sequences were identified and removed using UCHIME. The taxonomy of each 16S rRNA gene sequence was analyzed by RDP Classifier (http://rdp.cme.msu.edu/) against the silva (SSU115)16S rRNA database using confidence threshold of 70%.

2.10 In situ hybridization

Coronal brain sections (14 μm) sections were collected from Bregma +0.14mm to -2.92mm according to a standard mouse brain atlas [36]. The hybridization procedures and mRNA quantification were described in our previous study [37] (see Supporting Information for detailed methods).

2.11 Statistical analysis

Data were analyzed using the statistical package SPSS (version 20, IBM Corporation, Chicago, IL, USA). Data was first tested for normality before differences among the DIO, DR and LC groups were determined using one-way analysis of variance (ANOVA). This was followed by the post hoc Tukey-Kramer honestly significant difference (HSD) test for multiple comparisons among the groups. A p value of <0.05 was considered to be statistically significant. Values were

expressed as mean ± SEM. Pearson's correlations were used to examine the relationships between the parameters in the behavior tests and Bacteroidetes as well as plasma LPS and tight junction proteins in colon.

3 Results:

3.1 Chronic PA diet increased body weight, adiposity, food intake, and hepatic injury in DIO mice

On a chronic high PA diet, the DIO mice gained significantly more body weight than the DR and LF mice from 5 weeks and this persisted throughout the rest of the dietary intervention (Fig. 1A). The final body weight of DIO mice was 48% and 54% heavier than that of DR and LF mice (both $P < .01$) (Fig. 1B). Moreover, DIO mice consumed significantly more calories compared to the DR ($P < .05$) and LF mice ($P < .05$) (Fig. 1C). The DIO mice had higher inguinal, epididymal, perirenal and mesenteric fat masses compared to DR and LF mice (Fig. 1D). Furthermore, the DIO mice also had higher fat ratios after normalized to body weight (Fig. 1E). The IPGTT revealed that the DIO mice had an impaired glucose tolerance (Fig. 1F). The blood glucose levels of DIO mice significantly increased at 0, 15, 30, 60, and 120 minutes during the IPGTT compared to the DR and LF mice (All $P < .05$). Leptin and adiponectin are secreted from adipose tissue and have anti-obesity effects [38], but the DIO mice exhibited hyperleptinemia and a low ratio of plasma adiponectin to visceral fat (Fig. 1G-I), suggesting leptin resistance and impaired secretion of adiponectin in

these mice. Therefore, even though the DIO and DR mice were exposed to the same obesogenic diet and housed under the same conditions, the results suggest some genetic variations that contribute to the susceptibility of gaining weight on a high saturated-fat diet.

3.2 Chronic PA diet-induced DIO and DR mice have different gut microbiota profiles

Bacterial communities within the feces were determined by Illumina MiSeq sequencing of 16S rRNA genes and resulted in the recovery of 1604,201 effective sequences with a read length $\geqslant$ 360 bp. After quality filtering by QIIME, 1497,652 high-quality reads were obtained, accounting for 93.36% of the raw reads.

Out of the 318 bacterial species-level operational taxonomic units (OTUs) found in this study, 295 were found in LF and DR mice; only 272 were found in DIO mice. There were 252 OTUs shared by LF, DR and DIO groups. There were 23 OTUs shared by LF and DR mice, while there were only 6 OTUs shared by LF and DIO mice and 11 OTUs shared by DIO and DR mice (Fig. 2A). Furthermore, DIO mice had lower species richness than DR and LF mice [Chao 1 index (OTUs), DIO: 176.75±10.18, DR: 203.10±11.04; LF: 210.45±11.31, $P < .05$)]; and had lower species diversity than that of DR and LF mice [Shannon index (OTUs), DIO: 3.05 ± 0.34; DR: 4.07 ± 0.38; LF: 4.05 ± 0.37, $P < .05$] (Fig 2B). There was no significant difference in Chao1 and Shannon indices between LF and DR mice.

At the phyla level, the abundance of Firmicutes was higher in DIO mice compared to DR and LF mice ($P < .05$, Fig 2C), while there was no significant difference between DR and LF mice. The abundance of Bacteroidetes was lower in DIO and DR mice compared with LF mice, while DIO mice had a lower abundance than that of DR mice ($P < .05$, Fig 2C), suggesting that Bacteroidetes was not only decreased in obesity, also decreased by HF diet in DR mice without significant body weight gain. Similarly, the ratio of Firmicutes to Bacteroidetes in DIO mice and DR mice was significantly higher than LF mice (both $P < .05$, Fig 2D), while the DIO mice had the highest ratio. The abundance of Antinobacteria in DIO mice and DR mice were significantly higher than that of LF mice (both $P < .05$, Fig 2E) with the highest level in DIO mice. The abundance of Proteobacteria was lower in DIO group, but higher in the DR group compared to that of the LF group (both $P < .05$, Fig 2E).

When comparing the microbiota of DIO, DR and LF mice using LDA effect size (LEfSe) calculation, we found 30 differentially abundant taxonomic classes ($P < .05$) with an LDA score higher than 2.0 (Fig 2F). The results showed that phylum Actinobacteria, class Actinobacteria, order Bifidobacteriales, family Bifidobacteriaceae and genus Bifidobacterium were all significantly increased in DIO mice. Notably, bacteria belonging to order Clostridiales Ruminococcaceae_nk4a214_group, Family_XIII_AD3011_group and Family_XIII were increased significantly in DR mice and an unidentified genus of family Erysipelotrichaceae was also increased significantly in DR mice ($P < .05$, Fig 2F).

3.3 Chronic PA diet altered colonic tight junction protein expression and induced hyperendotoxinemia in DIO, but not DR mice.

To further determine whether changes in the gut microbiota could be associated with the epithelial permeability and systemic inflammation, we measured levels of tight junction protein expression and the plasma concentration of LPS, a trigger of inflammation. The epithelial cells in the colon are tightly bound by intercellular junctional protein complexes, occludin and zonula occludens (ZO-1), which regulate paracellular permeability and are crucial for the integrity of the epithelial barrier [39]. Both occludin and ZO-1 expression decreased significantly in the colon of DIO mice compared to DR and LF mice (all $P < .01$; Fig. 3A and B). Next, we found that the level of serum LPS significantly increased in DIO mice compared to DR and LF mice (both $P < .01$; Fig. 3C). There were significant negative associations between levels of serum LPS and the concentrations of occludin ($r = -0.631$, $p = 0.005$) and ZO-1 ($r = -0.929$, $P < .001$) (Fig. 3D and E), suggesting hyperendotoxinemia in DIO mice was associated with impaired tight junction in the colon.

3.4 Chronic PA diet induced inflammation in the colon of DIO but not DR mice.

It is known that inflammation increases intestinal epithelial tight junction permeability [40]. As levels of tight junction protein expression was reduced in the DIO mice in the present study, we further examined macrophage infiltration and inflammatory response in the colon of these mice. The positive immunoreactivity of F4/80 was significantly increased in the colon of DIO mice compared to DR and LF

mice (both p <0.01; Fig. 4A and B). Furthermore, we characterized the type of macrophages present. CD11c was used to detect M1 macrophages, which produce pro-inflammatory cytokines, and CD206 was used to detect M2 macrophages, which produce anti-inflammatory cytokines. The DIO mice had increased CD11c positive staining in the colon compared to DR and LF mice (both p <0.05; Fig. 4 A and C). There was no significant difference in CD206 staining among the DIO, DR and LF mice (Fig. 4 A and D). This indicates that the high PA diet promotes a shift in a pro-inflammatory M1 polarization in the colon of obese mice.

As the pro-inflammatory M1 macrophage is TLR4-responsive and often associated with low grade inflammation in local tissue, we measured the expression of TLR4 and its adaptor protein, MyD88, as well as downstream signaling molecules (NFκB, IκBα and pIκBα) and pro-inflammatory cytokines (tumor necrosis factor-α (TNF-α), interleukin-1β (IL-1β) and interleukin-6 (IL-6)) in the colon by Western blotting. The levels of TLR4 and MyD88 were higher in DIO mice than that of DR and LF mice (all p <0.05; Fig. 4E and G). NFκB and pIκBα significantly increased in DIO mice compared to DR and LF mice, while IκBa decreased in the colon of DIO mice. The levels pro-inflammatory cytokines, TNFα, IL-1β and IL-6, were higher in DIO mice than the DR and LF mice (all P < .05; Fig. 4F and H). In the colon tissue, the level of cyclooxygenase isoform 2 (COX-2, a pro-inflammatory marker implicated in colorectal cancer progression [41]) was increased in DIO mice, but not DR mice compared to LF mice (both P < .05; Fig. 4F and H).

3.5 Chronic PA diet induced hepatic inflammation in the DIO but not DR mice.

It has been reported that LPS binds to LPS-binding proteins in the liver, which then facilitate its transfer to CD14 receptors on the surface of the macrophages and activate the TLR4 signaling pathway [42]. Therefore, we examined hepatic pro-inflammatory signaling molecules in the DIO and DR mice. Firstly, the liver weight was heavier in DIO mice compared to DR and LF mice (both $P < .01$; Fig. 5A and B), and the ratio of liver weight to body weight was higher in DIO mice compared to DR and LF mice (both $P < .05$; Fig. 5C). Furthermore, At a histological level, the diagnostic criteria for hepatic steatosis includes the presence of steatosis and ballooning [43]. H & E staining revealed that the hepatocytes of DIO mice were enlarged and contained large cytoplasmic lipid droplets compared to the DR group (ballooning: + 274%, $P < .001$; steatosis: + 361%, $P < .001$) and LF mice (ballooning: + 319%, $P < .001$; steatosis: + 391%, $P < .001$) (Fig. 5D and E). Moreover, the levels of TLR4, MyD88 and NFκB (inflammatory signaling molecules) were increased in the liver of DIO mice compared to DR and LF mice, while there was no significant difference between DR and LF mice (Fig. 5F and G). Therefore, DIO mice exhibited hepatic inflammation and steatosis, symptoms reportedly associated with insulin resistance and glucose intolerance [44]; the latter of which was also observed in these mice (see Section 3.1).

3.6 Chronic PA diet impaired cognitive function in DIO mice and reduced hippocampal BDNF expression

Studies show that cognition and BDNF levels are affected by alterations to gut microbiota [27, 28]. Therefore, we examined recognition and spatial memory, and

hippocampal BDNF levels in DIO mice (ie in the presence of concurrent altered gut microbiota). In the Y maze test, spatial memory was impaired in DIO mice, who showed a significant reduction in the ratio of time spent in the novel arm compared to the LF and DR mice (both $P < .05$; Fig. 6A). In novel object recognition test, the DIO mice showed a significant reduction in the discrimination index compared with LF and DR mice (both $P < .01$; Fig. 6B), suggesting the impairment of recognition memory. Recent studies have demonstrated a clear association between changes in microbiota and cognitive behavior [45]. Here, the Pearson's correlation analysis revealed a significant positive correlation between the abundance of Bacteroidetes and cognitive behavior, including the ratio of time spent in novel arm ($r = 0.65$, $p = 0.003$) and discrimination index ($r = 0.80$, $P < .001$) (Fig. 6C and D). Next, in-situ hybridization was used to examine the level of hippocampal BDNF mRNA expression, which is implicated in spatial and recognition memory. The level of BDNF mRNA expression was significantly decreased in the hippocampus, including the CA1-3 and DG regions, in DIO mice compared to DR and LF mice ($P < .05$; Fig. 6E and F).

4 DISCUSSION

In this study, we found that some mice developed obesity whilst others were diet-resistant and remained lean when fed the same chronic high PA diet. There was a significant reduction in gut microbiota richness and diversity in the DIO mice, but not the DR mice. DIO mice had reduced tight junction protein expression, increased plasma LPS and increased inflammation in colon and liver. The gut microbiota (e.g. Bacteroidetes) is important for cognitive function [46]; in this study, we found that recognition and spatial memory were impaired in the DIO mice, with concurrent decreased abundance of Bacteroidetes and hippocampal BDNF mRNA expression.

On the other hand, the DR mice did not exhibit changes in colonic tight junction protein expression, levels of plasma LPS, inflammatory response in the colon and liver, or cognitive performance, although minor alterations in some gut microbiota at phylum level were observed compared to the LF controls.

In the present study, we found that the richness (Chao1 index) of gut microbiota was decreased in the DIO, but not in the DR mice. This is consistent with a human study in which individuals with a low bacterial richness exhibited more adiposity, as well as insulin resistance and dyslipidaemia, and a more pronounced inflammatory phenotype compared to individuals with a high bacterial richness [16]. Furthermore, the study found that obese individuals with the lower bacterial richness also gained more weight over a 9 year period compared to subjects with a high bacterial richness. Therefore, our results, combined with the human findings[16], provide evidence that alterations in our second genome - the gut microbiota - may contribute to the heterogeneity associated with adiposity-related phenotypes. Furthermore, the diversity (Shannon index) of gut microbiota was decreased in the DIO mice. At the phylum level, the abundance of Gram-negative Bacteroidetes and Proteobacteria were decreased in DIO mice. Interestingly, in DR mice, the abundance of Bacteriodetes was also decreased, but Proteobacteria was increased compared to the LF control mice. LPS is a major component of the outer layer of Gram-negative bacteria and plasma LPS levels are closely correlated with the Gram-negative Bacteroides-like intestinal bacteria [47]. An elevated level of plasma LPS was previously related to the over-production of LPS in the gut by the death of Gram-negative bacteria and their

translocation into the blood circulation [47, 48]. In the present study, the plasma LPS increased in DIO mice, but not in DR mice, suggesting that endotoximia in obesity may result from the dysbiosis of Gram-negative bacteria (specifically, a decrease in both Bacteroidetes and Proteobacteria), while an increased proportion of Proteobacteria in DR mice may, to some degree, compensate for decreased levels of Bacteroidetes.

Furthermore, we found that DIO mice consumed more calories. The reason of DIO mice consumes more calories could be due to multiple factors. It could be due altered regulation of gut-brain axis induced by an interaction of genetic and environment factors (such as high-fat diet). For example, previously we found that in DIO mice there is decreased gut anorexigenic peptide YY (PYY)-central neuropeptide Y (NPY) Y2 receptor axis, which plays an important role in promoting negative energy balance regulation[49]. Furthermore, Y2 receptor binding is also lowered in the hypothalamus in DIO mice when their body weight is similar as DR mice with energy restriction diet, suggesting a possible intrinsic nature of the DIO mice in response to high-fat diet.

Furthermore, we found that expression of the tight junction proteins, occludin and ZO-1, decreased in the colon of DIO mice. The tight junction protein complex seals the paracellular space between epithelial cells, thus preventing paracellular diffusion of luminal microorganisms and their fragments, such as LPS. In the present study, there was a negative correlation between the levels of hyperendotoxinemia and tight junction proteins, occludin and ZO-1, in the colon. Furthermore, levels of

pro-inflammatory M1 macrophages stained with CD11c were increased in the colon of DIO mice without a concurrent alteration in anti-inflammatory M2 macrophage (CD206-positive) levels. Our finding indicates there is a shift in macrophage subtype to a pro-inflammatory M1 polarization in the colon of high palmitic acid diet-induced obesity. To our knowledge, it is firstly to report a M1 macrophage shift in the colon during obesity induced by high palmitic acid diet. It has been reported that anti-inflammatory M2 macrophages can shift into M1 macrophages to promote inflammation following LPS stimulation [50]. Therefore, the hyperendotoxinemia in DIO mice may contribute to the M1 pro-inflammatory macrophage shift in colon, in which most resident macrophages are normally M2 expressing CD206 to prevent inflammation [51].

TLR4 receptors are highly expressed in the colon compared to other parts of the intestine [18, 19]. Not only does LPS activate the TLR4 receptor, but palmitic acid also interacts with this receptor [52]. In the present study, TLR4 levels were elevated in the colon tissue of DIO mice. Therefore, an abundance of palmitic acids in the colon and over production of LPS from the microbiota may activate TLR4 in colon in the DIO mice. TLR4-MyD88-dependent pathway activates IκB-NFκBβ [20]. NFκB, a transcription factor, can promote the transcription of pro-inflammatory genes, such as IL-6 and TNFα, which in-turn can directly propagate tumorigenesis. In the colon, TLR4 expression is associated with adenocarcinoma and increased risk of disease progression. Saturated fatty acids modulate TLR4-mediated NFκB signaling pathways and increase COX2 [53], which plays important roles in inflammation and cancer

progression [47]. Epidemiological data suggest that obesity is associated with a 30-70% increased risk of colon cancer in human [54]. Previously, we have reported that DIO mice develop colon polyps at a rate 2.5 times greater than the DR mice [55]. Therefore, activation of TLR4 and its downstream signaling pathway MyD88-NFκB in the colon tissue may contribute to colonic inflammation and polyp formation and obesity-related colon cancer.

In the present study, the use of a novel object recognition test and exploration of a Y-maze demonstrated that recognition and spatial memory were impaired in high-palmitic acid induced obese mice (DIO), in which hippocampal BDNF levels were also decreased. Previous studies have highlighted a link between BDNF, microbiota and cognition behavior. For example, cognitive dysfunction is apparent in mice exhibiting altered hippocampal BDNF levels following an induced enteric infection, ~30 days post-inoculation [27]. Moreover, intraperitoneal administration of LPS in mice leads to reduced hippocampal BDNF and cognitive defects [56]. In the present study, alterations to gut microbiota in diet-induced obesity might be responsible for the observed cognition decline. We found a correlation between decreased Bacteroidetes and alterations in cognitive behaviors, but proof of a direct cause and effect mechanism is still required. Nevertheless, this correlation is further supported by a recent study reporting that Bacteroides in the infant gut (at 1 year of age) has a role in cognitive development and brain morphometry [46]. A higher abundance of Bacteroides at 1 year of age has been correlated with a higher cognitive ability (based on an overall composite score), as well as improved expressive

language subscale when measured again at age 2 years of age [46]. However, further studies on the gut microbiota-brain axis in diet-induced obesity are required. For example, future studies could examine cognitive behavior in normal weight, LF diet mice following transplantation of fecal microbiota obtained from palmitic-acid diet-induced obese mice, or whether supplementation of Bacteroide-rich microbiota can improve cognition in diet-induced obese mice.

In conclusion, this study has showed that a diet high in obesogenic palmitic acid induced some mice to become obese, while others remained lean, despite being fed the same diet. The response in microbiota, colon and brain of diet-induced obesity was investigated in mice prone and resistant to obesogenic diet. The obese mice had decreased richness and diversity of gut microbiota, a pro-inflammatory M1 macrophage shift and impaired tight junctions between epithelial cells of the colon, with an ensuing increase in plasma levels of the endotoxin, LPS. In addition, recognition and spatial memory were impaired in obese mice, with concurrently reduced hippocampal BDNF levels. Conversely, there were no significant alterations in colonic tight junction proteins, plasma LPS, colonic inflammation, or cognitive performance in mice resistant to obesity compared to lean (LF-diet) mice. Taken together, these data suggest that gut microbiota, colon inflammation and LPS may play a major role in the development of the obese phenotype and cognitive decline in high palmitic acid diet-induced obesity. Furthermore, this study did not examine microbiome prior to obesity phenotype which will be our future study.

ACKNOWLEDGEMENTS

We wish to acknowledge the University of Wollongong and Illawarra Health and Medical Research Institute for financially supporting the experimental works. This study was also supported by a Diabetes Australia Research Trust Research Project (Y12G-YUYI) awarded to Dr. YH Yu. We are grateful for support for this study from the Priority Academic Program Development of Jiangsu Higher Education Institutions (PAPD), Dean Special Foundation of Xuzhou Medical University (2012KJZ07), General Financial Grant from the Chinese Postdoctoral Science Foundation (2014M561713) and The Program for Youth Science and Technology Innovative Research Team of Xuzhou Medical University. *XFH* and *KZ* conceived and designed the studies; *PZ, YY, YQ, YZ, QW, XL,* and *HW* performed the studies and analysed the data; *YY, PZ,* KW *and XFH* wrote the manuscript.

Disclosure statement

The authors have no actual or potential conflicts of interest to report.

REFERENCES:

[1] Yu Y, Cai Z, Zheng J, Chen J, Zhang X, Huang XF, et al. Serum levels of polyunsaturated fatty acids are low in Chinese men with metabolic syndrome, whereas serum levels of saturated fatty acids, zinc, and magnesium are high. Nutr Res. 2012;32:71-7.
[2] Kabagambe EK, Tsai MY, Hopkins PN, Ordovas JM, Peacock JM, Borecki IB, et al. Erythrocyte fatty acid composition and the metabolic syndrome: a National Heart, Lung, and Blood Institute GOLDN study. Clin Chem. 2008;54:154-62.
[3] Speakman JR. Obesity: the integrated roles of environment and genetics. The Journal of nutrition. 2004;134:2090s-105s.
[4] Xin XG, Storlien LH, Huang XF. Hypothalamic c-fos-like immunoreactivity in high-fat diet-induced obese and resistant mice. Brain Res Bull. 2000;52:235-42.
[5] Lin S, Thomas TC, Storlien LH, Huang XF. Development of high fat diet-induced obesity and leptin resistance in C57Bl/6J mice. International journal of obesity and related metabolic disorders : journal of the International Association for the Study of Obesity. 2000;24:639-46.
[6] Lauterio TJ, Bond JP, Ulman EA. Development and characterization of a purified diet to identify obesity-susceptible and resistant rat populations. J Nutr. 1994;124:2172-8.
[7] Gorski JN, Dunn-Meynell AA, Levin BE. Maternal obesity increases hypothalamic leptin receptor expression and sensitivity in juvenile obesity-prone rats. Am J Physiol Regul Integr Comp Physiol. 2007;292:R1782-91.
[8] Koza RA, Rogers P, Kozak LP. Inter-individual variation of dietary fat-induced mesoderm specific transcript in adipose tissue within inbred mice is not caused by altered promoter methylation. Epigenetics. 2009;4:512-8.
[9] Koza RA, Nikonova L, Hogan J, Rim JS, Mendoza T, Faulk C, et al. Changes in gene expression foreshadow diet-induced obesity in genetically identical mice. Plos Genet. 2006;2:769-80.
[10] Levin BE. Developmental gene x environment interactions affecting systems regulating energy homeostasis and obesity. Front Neuroendocrinol. 2010;31:270-83.
[11] Ley RE, Backhed F, Turnbaugh P, Lozupone CA, Knight RD, Gordon JI. Obesity alters gut microbial ecology. Proc Natl Acad Sci U S A. 2005;102:11070-5.
[12] Ley RE, Turnbaugh PJ, Klein S, Gordon JI. Microbial ecology: human gut microbes associated with obesity. Nature. 2006;444:1022-3.
[13] Tilg H, Kaser A. Gut microbiome, obesity, and metabolic dysfunction. The Journal of clinical investigation. 2011;121:2126-32.
[14] Schwiertz A, Taras D, Schafer K, Beijer S, Bos NA, Donus C, et al. Microbiota and SCFA in Lean and Overweight Healthy Subjects. Obesity. 2010;18:190-5.
[15] Turnbaugh PJ, Backhed F, Fulton L, Gordon JI. Diet-induced obesity is linked to marked but reversible alterations in the mouse distal gut microbiome. Cell Host Microbe. 2008;3:213-23.
[16] Erridge C, Attina T, Spickett CM, Webb DJ. A high-fat meal induces low-grade endotoxemia: evidence of a novel mechanism of postprandial inflammation. Am J Clin Nutr. 2007;86:1286-92.
[17] Yu Z, Tang L, Chen L, Li J, Wu W, Hu C. Capillarisin Suppresses Lipopolysaccharide-Induced Inflammatory Mediators in BV2 Microglial Cells by

Suppressing TLR4-Mediated NF-kappaB and MAPKs Signaling Pathway. Neurochem Res. 2015;40:1095-101.
[18] Wang YW, Devkota S, Musch MW, Jabri B, Nagler C, Antonopoulos DA, et al. Regional Mucosa-Associated Microbiota Determine Physiological Expression of TLR2 and TLR4 in Murine Colon. Plos One. 2010;5.
[19] Ortega-Cava CF, Ishihara S, Rumi MAK, Kawashima K, Ishimura N, Kazumori H, et al. Strategic compartmentalization of toll-like receptor 4 in the mouse gut. J Immunol. 2003;170:3977-85.
[20] Baker RG, Hayden MS, Ghosh S. NF-kappaB, inflammation, and metabolic disease. Cell Metab. 2011;13:11-22.
[21] Lee SH, Starkey PM, Gordon S. Quantitative analysis of total macrophage content in adult mouse tissues. Immunochemical studies with monoclonal antibody F4/80. J Exp Med. 1985;161:475-89.
[22] Bain CC, Mowat AM. Macrophages in intestinal homeostasis and inflammation. Immunol Rev. 2014;260:102-17.
[23] Mowat AM, Agace WW. Regional specialization within the intestinal immune system. Nature reviews Immunology. 2014;14:667-85.
[24] Lumeng CN, Bodzin JL, Saltiel AR. Obesity induces a phenotypic switch in adipose tissue macrophage polarization. The Journal of clinical investigation. 2007;117:175-84.
[25] Kawano Y, Nakae J, Watanabe N, Kikuchi T, Tateya S, Tamori Y, et al. Colonic Pro-inflammatory Macrophages Cause Insulin Resistance in an Intestinal Ccl2/Ccr2-Dependent Manner. Cell Metab. 2016;24:295-310.
[26] Ray I, Mahata SK, De RK. Obesity: An Immunometabolic Perspective. Frontiers in Endocrinology. 2016;7.
[27] Gareau MG, Wine E, Rodrigues DM, Cho JH, Whary MT, Philpott DJ, et al. Bacterial infection causes stress-induced memory dysfunction in mice. Gut. 2011;60:307-17.
[28] Bercik P, Denou E, Collins J, Jackson W, Lu J, Jury J, et al. The Intestinal Microbiota Affect Central Levels of Brain-Derived Neurotropic Factor and Behavior in Mice. Gastroenterology. 2011;141:599-U701.
[29] Yu YH, South T, Wang Q, Huang XF. Differential expression of hypothalamic CART mRNA in response to body weight change following different dietary interventions. Neurochem Int. 2008;52:1422-30.
[30] Huang XF, Han M, Storlien LH. The level of NPY receptor mRNA expression in diet-induced obese and resistant mice. Mol Brain Res. 2003;115:21-8.
[31] Camer D, Yu Y, Szabo A, Dinh CH, Wang H, Cheng L, et al. Bardoxolone methyl prevents insulin resistance and the development of hepatic steatosis in mice fed a high-fat diet. Mol Cell Endocrinol. 2015;412:36-43.
[32] Wang S, Huang XF, Zhang P, Wang H, Zhang Q, Yu S, et al. Chronic rhein treatment improves recognition memory in high-fat diet-induced obese male mice. The Journal of nutritional biochemistry. 2016;36:42-50.
[33] Duffy L, Cappas E, Lai D, Boucher AA, Karl T. Cognition in transmembrane domain neuregulin 1 mutant mice. Neuroscience. 2010;170:800-7.
[34] Dinh CH, Yu Y, Szabo A, Zhang Q, Zhang P, Huang XF. Bardoxolone Methyl Prevents High-Fat Diet-Induced Colon Inflammation in Mice. The journal of

histochemistry and cytochemistry : official journal of the Histochemistry Society. 2016;64:237-55.
[35] Zhang Q, Yu Y, Huang XF. Olanzapine Prevents the PCP-induced Reduction in the Neurite Outgrowth of Prefrontal Cortical Neurons via NRG1. Sci Rep-Uk. 2016;6:19581.
[36] Paxinos G, Franklin KBJ. The Mouse Brain in Stereotaxic Coordinates, 1st edn., Academic Press, San Diego. 2002.
[37] Wong JY, Liberatore GT, Donnan GA, Howells DW. Expression of brain-derived neurotrophic factor and TrkB neurotrophin receptors after striatal injury in the mouse. Experimental Neurology. 1997;148:83-91.
[38] Stern Jennifer H, Rutkowski Joseph M, Scherer Philipp E. Adiponectin, Leptin, and Fatty Acids in the Maintenance of Metabolic Homeostasis through Adipose Tissue Crosstalk. Cell Metab.23:770-84.
[39] Ulluwishewa D, Anderson RC, McNabb WC, Moughan PJ, Wells JM, Roy NC. Regulation of Tight Junction Permeability by Intestinal Bacteria and Dietary Components. The Journal of nutrition. 2011;141:769-76.
[40] Al-Sadi RM, Ma TY. IL-1beta causes an increase in intestinal epithelial tight junction permeability. J Immunol. 2007;178:4641-9.
[41] Wang D, DuBois RN. The role of COX-2 in intestinal inflammation and colorectal cancer. Oncogene. 2009;29:781-8.
[42] Su GL. Lipopolysaccharides in liver injury: molecular mechanisms of Kupffer cell activation. Am J Physiol-Gastr L. 2002;283:G256-G65.
[43] Neuschwander-Tetri BA, Caldwell SH. Nonalcoholic steatohepatitis: summary of an AASLD Single Topic Conference. Hepatology. 2003;37:1202-19.
[44] Perry RJ, Samuel VT, Petersen KF, Shulman GI. The role of hepatic lipids in hepatic insulin resistance and type 2 diabetes. Nature. 2014;510:84-91.
[45] Gareau MG. Microbiota-gut-brain axis and cognitive function. Advances in experimental medicine and biology. 2014;817:357-71.
[46] Carlson AL, Xia K, Azcarate-Peril A, Goldman BD, Styner MA, Thompson AL, et al. Variation in the infant gut microbiome is associated with cognitive development and brain morphometry. Annual Meeting of the American College of Neuropsychopharmacology, ACNP 20162016.
[47] Cani PD, Amar J, Iglesias MA, Poggi M, Knauf C, Bastelica D, et al. Metabolic endotoxemia initiates obesity and insulin resistance. Diabetes. 2007;56:1761-72.
[48] Neal MD LC, Levy R, Prince J, Billiar TR, Watkins S, Li J, Cetin S, Ford H, Schreiber A, Hackam DJ. Enterocyte TLR4 mediates phagocytosis and translocation of bacteria across the intestinal barrier. J Immunol. 2006.
[49] Rahardjo GL, Huang XF, Tan YY, Deng C. Decreased plasma peptide YY accompanied by elevated peptide YY and Y2 receptor binding densities in the medulla oblongata of diet-induced obese mice. Endocrinology. 2007;148:4704-10.
[50] Zheng XF, Hong YX, Feng GJ, Zhang GF, Rogers H, Lewis MAO, et al. Lipopolysaccharide-Induced M2 to M1 Macrophage Transformation for IL-12p70 Production Is Blocked by Candida albicans Mediated Up-Regulation of EBI3 Expression. Plos One. 2013;8.
[51] Bain CC, Scott CL, Uronen-Hansson H, Gudjonsson S, Jansson O, Grip O, et al. Resident and pro-inflammatory macrophages in the colon represent alternative

context-dependent fates of the same Ly6C(hi) monocyte precursors. Mucosal Immunol. 2013;6:498-510.
[52] Eguchi K, Manabe I, Oishi-Tanaka Y, Ohsugi M, Kono N, Ogata F, et al. Saturated Fatty Acid and TLR Signaling Link β Cell Dysfunction and Islet Inflammation. Cell Metab. 2012;15:518-33.
[53] Lee JY, Sohn KH, Rhee SH, Hwang D. Saturated Fatty Acids, but Not Unsaturated Fatty Acids, Induce the Expression of Cyclooxygenase-2 Mediated through Toll-like Receptor 4. J Biol Chem. 2001;276:16683-9.
[54] Bardou M, Barkun AN, Martel M. Obesity and colorectal cancer. Gut. 2013;62:933-47.
[55] Bocarsly ME, Fasolino M, Kane GA, LaMarca EA, Kirschen GW, Karatsoreos IN, et al. Obesity diminishes synaptic markers, alters microglial morphology, and impairs cognitive function. P Natl Acad Sci USA. 2015;112:15731-6.
[56] Richwine AF, Sparkman NL, Dilger RN, Buchanan JB, Johnson RW. Cognitive deficits in interleukin-10-deficient mice after peripheral injection of lipopolysaccharide. Brain Behav Immun. 2009;23:794-802.

FIGURE LEGENDS:

Fig. 1. (A) Body weight gain, (B) final body weight, (C) energy intake, (D) fat mass, (E) the ratio of fat pad weight to body weight, (F) intraperitoneal glucose tolerance test, (G) plasma leptin, (H) plasma adiponectin, and (I) ratio of adiponectin to visceral (Visc.) fat in diet-induced obese (DIO), diet-resistant (DR) and low-fat (LF) diet fed mice. * $P < .05$ vs. LF. $^{\#}$ $P < .05$ vs. DR. Values are mean ± SEM, n=18.

Fig. 2. The gut microbial communities in diet-induced obese (DIO), diet-resistant (DR) and low-fat (LF) diet fed mice. (A) Venn diagrams comparing the OTU memberships, (B) richness (Chao 1 index) and diversity (Shannon index) of gut microbial communities based on out, (C) abundance of Firmicutes and Bacteroidetes, (D) ratio of Firmicutes (FM) to Bacteroidetes (BO), (E) abundance of Antinobacteria and Proteobacteria, (F) LEfSe results on mice gut microbiomes. Values are mean ± SEM, n = 6. * $P < .05$ vs. LF. # $P < .05$ vs. DR.

Fig. 3. (A and B) Protein expression levels of occludin and zonula occludens-1 (ZO-1) in the colon, (C) plasma LPS levels, and correlations between plasma LPS levels and colonic (D) occludin or (E) ZO-1 expression in diet-induced obese (DIO), diet-resistant (DR) and low-fat (LF) diet fed mice. Values are mean ± SEM, n=6. * $P < .05$ vs. LF. $^{\#}$ $P < .05$ vs. DR.

Fig. 4. Inflammatory markers in the colon. (A) Immunohistochemical staining; percentage of (B) F4/80-, (C) CD11c- and (D) CD206-positive cells, (E and G) colonic

protein expression levels of TLR4, MyD88, NFκB, IκBα and p-IκBα, and (F and H) colonic protein expression levels of TNF-α, IL-1β, IL-6 and COX2, in diet-induced obese (DIO), diet-resistant (DR) and low-fat (LF) diet fed mice. Values are mean ± SEM, n=6. * $P < .05$ vs. LF. $^{\#}$ $P < .05$ vs. DR. Scale bar: 80 μM.

Fig. 5. (A) Fresh liver appearance, (B) liver weight, (C) liver weight / Body weight, (D) hematoxylin and eosin staining of liver, (E) index of hepatic steatosis and cellular ballooning, and (F and G) protein expression levels of TLR4, MyD88 and NFκB in the liver of diet-induced obese (DIO), diet-resistant (DR) and low-fat (LF) diet fed mice. Values are mean ± SEM, n=6. * $P < .05$ vs. LF. $^{\#}$ $P < .05$ vs. DR. Scale bar: 10 μM

Fig. 6. (A) The ratio of time spent in novel arm in the Y maze test, (B) discrimination index in the novel object recognition test, and correlation between levels of gut Bacteroidetes and (C) ratio of time spent in the novel arm or (D) discrimination index, and (E and F) hippocampal BDNF mRNA levels in diet-induced obese (DIO), diet-resistant (DR) and low-fat (LF) diet fed mice. Values are mean ± SEM, n=12 in (A) and (B); n=6 in (C, D, E, F). * $P < .05$ vs. LF. $^{\#}$ $P < .05$ vs. DR. Scale bar: 50 μM.

Fig 1

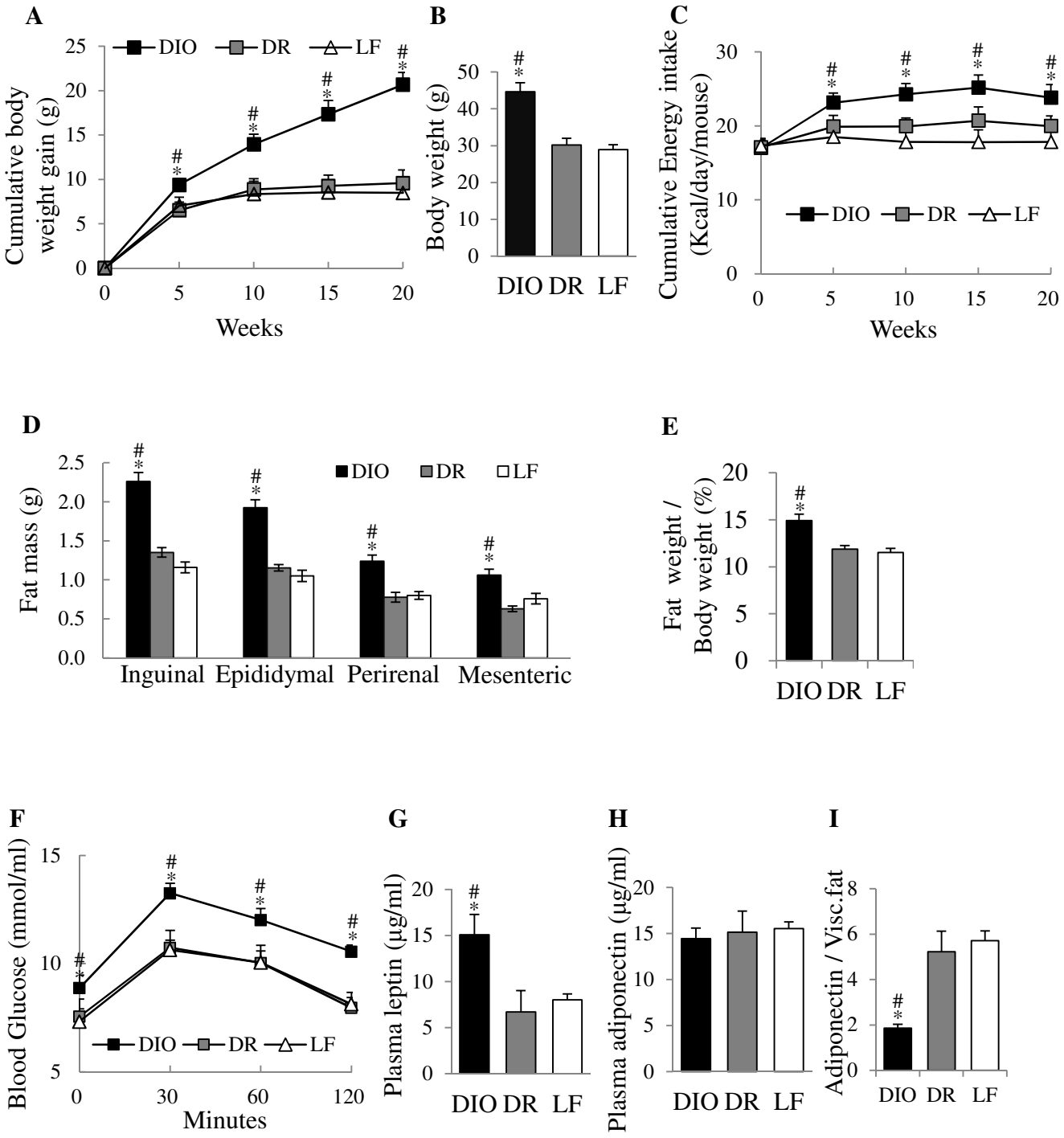
A
B
C
D
E
F
G
H
I
DIO
DR
LF
Cumulative body weight gain (g)
Weeks
Body weight (g)
Cumulative Energy intake (Kcal/day/mouse)
Fat mass (g)
Inguinal
Epididymal
Perirenal
Mesenteric
Fat weight / Body weight (%)
Blood Glucose (mmol/ml)
Minutes
Plasma leptin (μg/ml)
Plasma adiponectin (μg/ml)
Adiponectin / Visc.fat

Fig 2

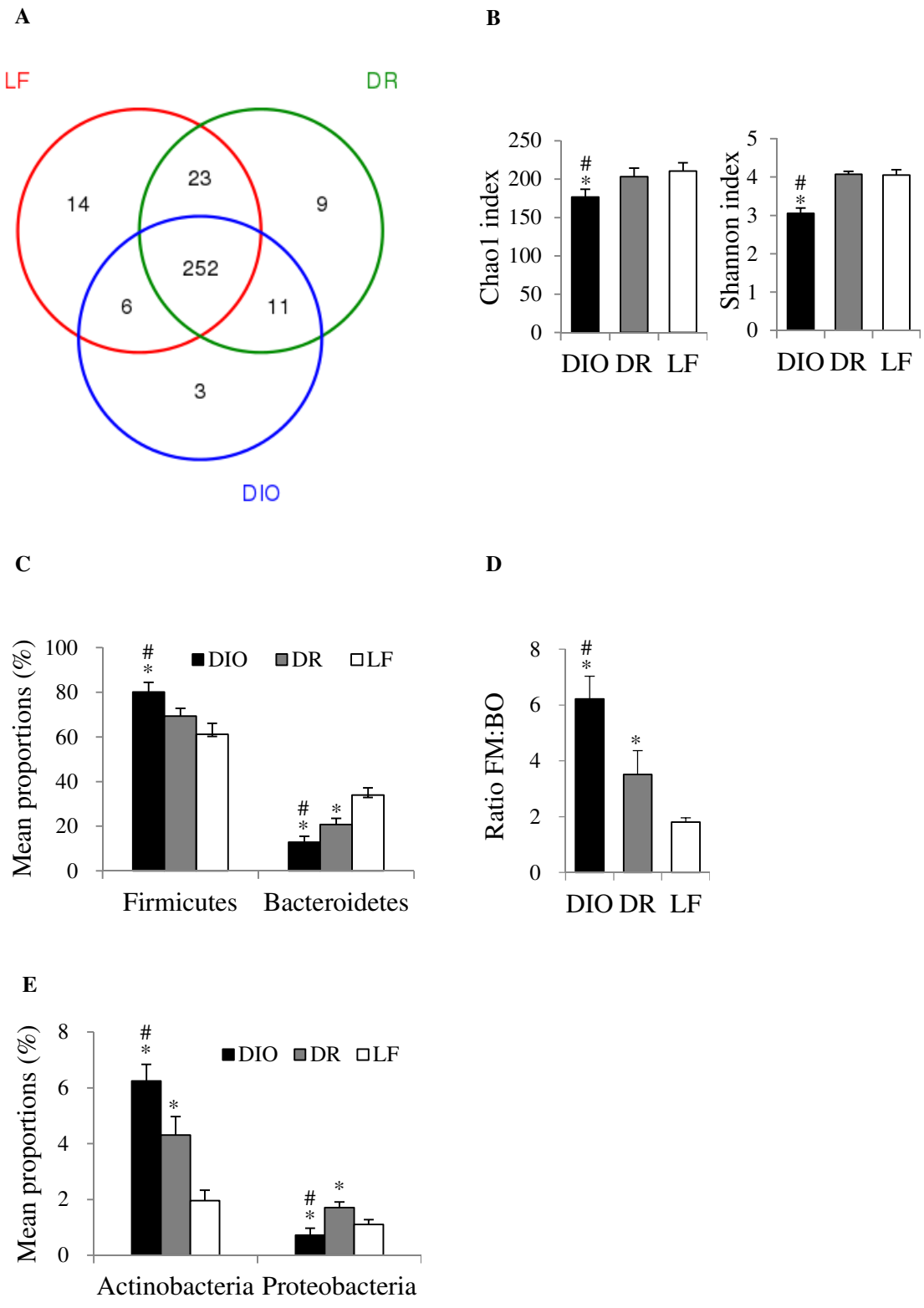
A
LF
DR
DIO
14
23
9
252
6
11
3
B
Chao1 index
250
200
150
100
50
0
DIO DR LF
Shannon index
5
4
3
2
1
0
DIO DR LF
C
Mean proportions (%)
100
80
60
40
20
0
DIO DR LF
Firmicutes
Bacteroidetes
D
Ratio FM:BO
8
6
4
2
0
DIO DR LF
E
Mean proportions (%)
8
6
4
2
0
DIO DR LF
Actinobacteria
Proteobacteria

F

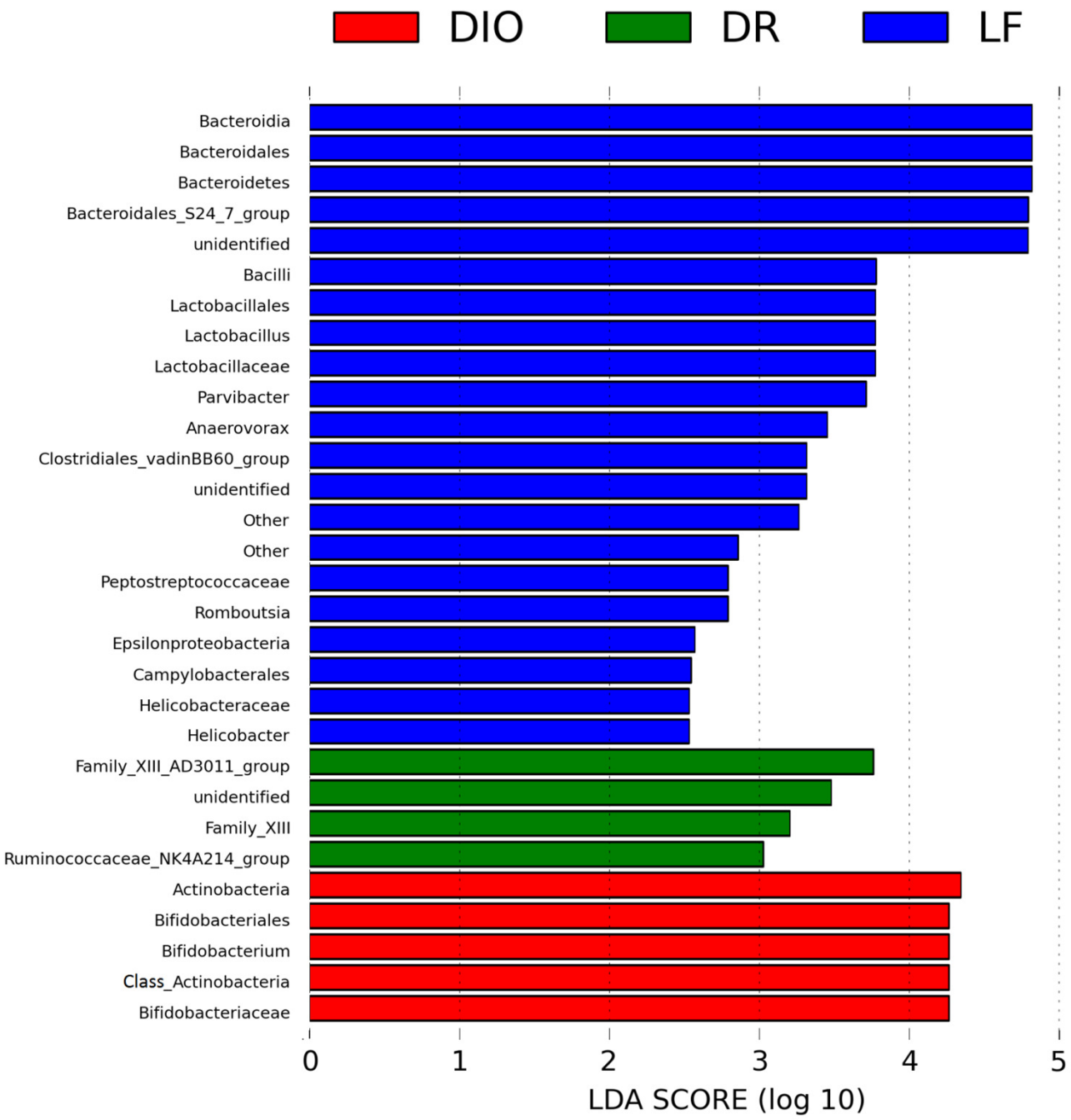
DIO
DR
LF
Bacteroidia
Bacteroidales
Bacteroidetes
Bacteroidales_S24_7_group
unidentified
Bacilli
Lactobacillales
Lactobacillus
Lactobacillaceae
Parvibacter
Anaerovorax
Clostridiales_vadinBB60_group
unidentified
Other
Other
Peptostreptococcaceae
Romboutsia
Epsilonproteobacteria
Campylobacterales
Helicobacteraceae
Helicobacter
Family_XIII_AD3011_group
unidentified
Family_XIII
Ruminococcaceae_NK4A214_group
Actinobacteria
Bifidobacteriales
Bifidobacterium
Class_Actinobacteria
Bifidobacteriaceae
0
1
2
3
4
5
LDA SCORE (log 10)

Fig 3

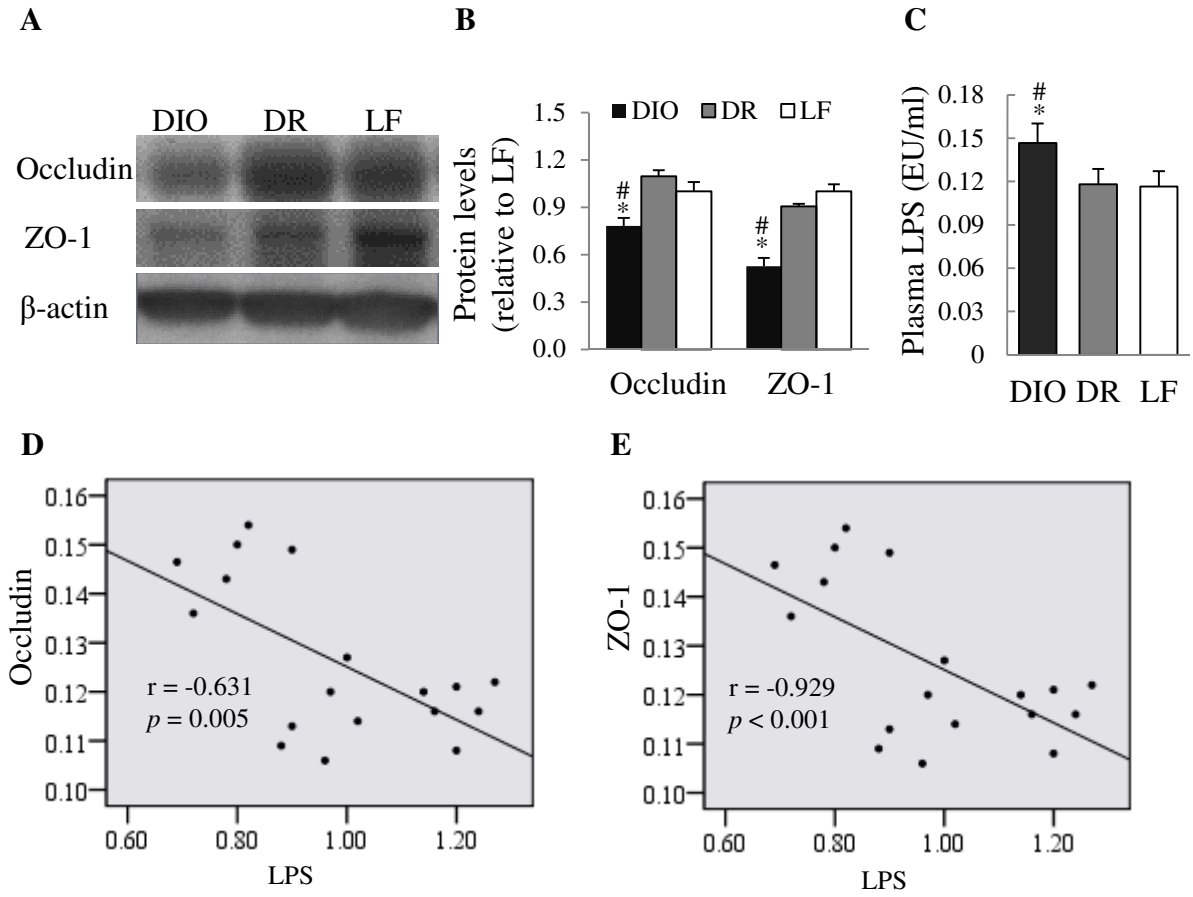
A
DIO
DR
LF
Occludin
ZO-1
β-actin
B
DIO
DR
LF
Protein levels (relative to LF)
1.5
1.2
0.9
0.6
0.3
0.0
#
*
#
*
Occludin
ZO-1
C
Plasma LPS (EU/ml)
0.18
0.15
0.12
0.09
0.06
0.03
0
#
*
DIO DR LF
D
Occludin
0.16
0.15
0.14
0.13
0.12
0.11
0.10
r = -0.631
p = 0.005
0.60
0.80
1.00
1.20
LPS
E
ZO-1
0.16
0.15
0.14
0.13
0.12
0.11
0.10
r = -0.929
p < 0.001
0.60
0.80
1.00
1.20
LPS

Fig 4

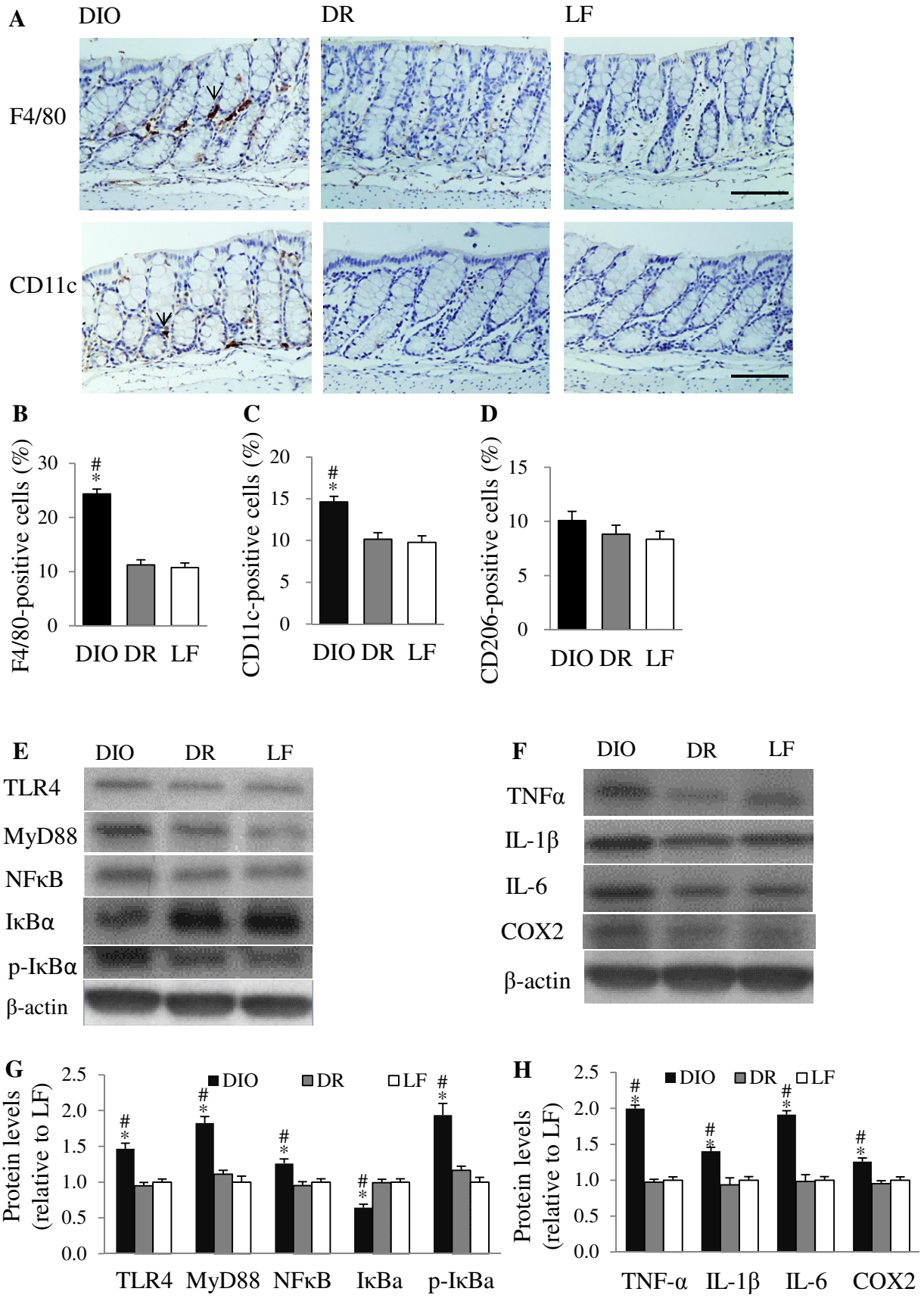
A
DIO
DR
LF
F4/80
CD11c
B
F4/80-positive cells (%)
30
20
10
0
DIO DR LF
C
CD11c-positive cells (%)
20
15
10
5
0
DIO DR LF
D
CD206-positive cells (%)
15
10
5
0
DIO DR LF
E
DIO
DR
LF
TLR4
MyD88
NFκB
IκBα
p-IκBα
β-actin
F
DIO
DR
LF
TNFα
IL-1β
IL-6
COX2
β-actin
G
Protein levels (relative to LF)
2.5
2.0
1.5
1.0
0.5
0.0
DIO
DR
LF
TLR4
MyD88
NFκB
IκBa
p-IκBa
H
Protein levels (relative to LF)
2.5
2.0
1.5
1.0
0.5
0.0
DIO
DR
LF
TNF-α
IL-1β
IL-6
COX2

Fig 5

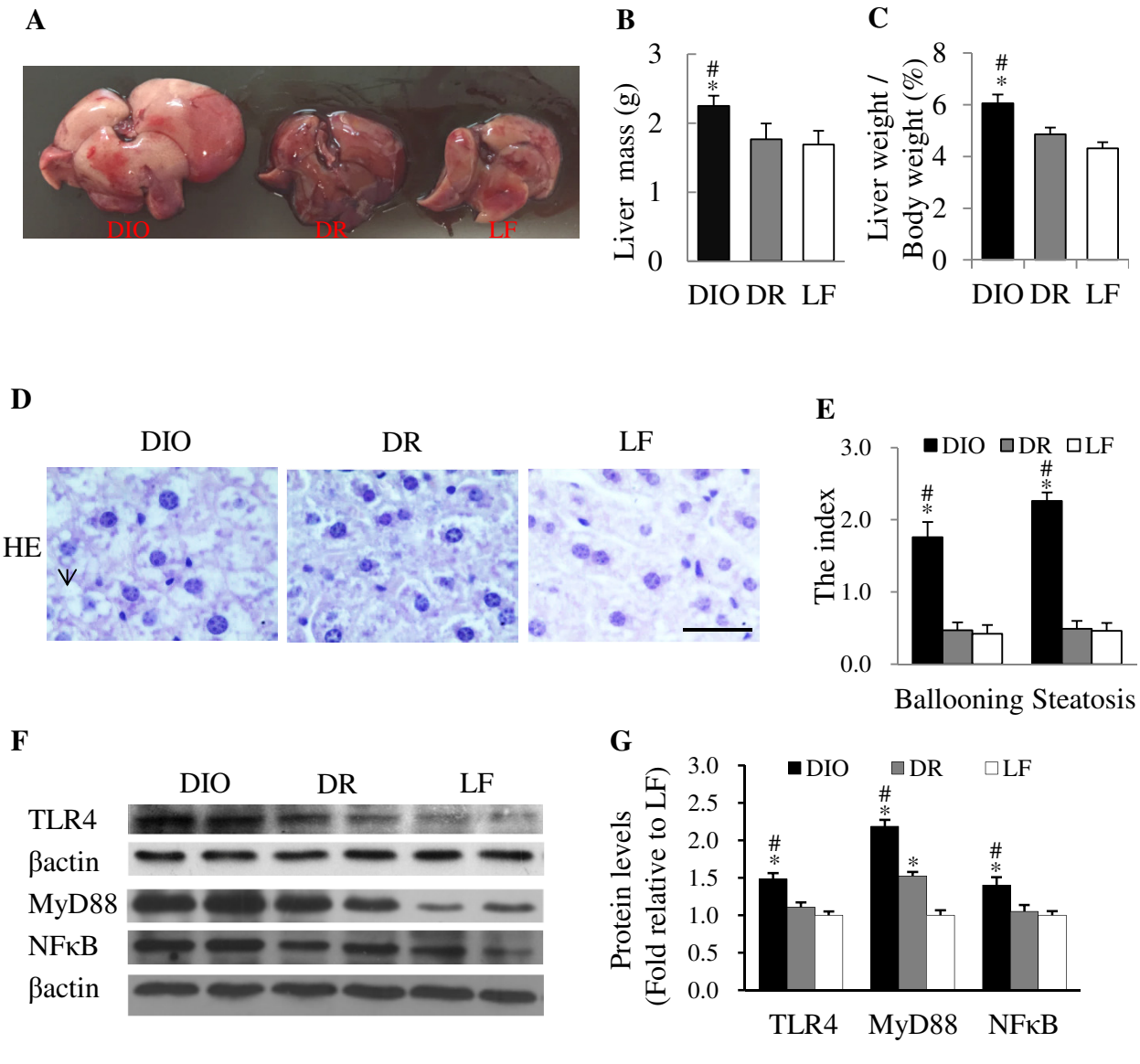
A
DIO
DR
LF
B
Liver mass (g)
3
2
1
0
#
*
DIO DR LF
C
Liver weight / Body weight (%)
8
6
4
2
0
#
*
DIO DR LF
D
DIO
DR
LF
HE
E
DIO
DR
LF
The index
3.0
2.0
1.0
0.0
#
*
#
*
Ballooning Steatosis
F
DIO
DR
LF
TLR4
βactin
MyD88
NFκB
βactin
G
DIO
DR
LF
Protein levels (Fold relative to LF)
3.0
2.5
2.0
1.5
1.0
0.5
0.0
#
*
#
*
*
#
*
TLR4
MyD88
NFκB

Fig 6

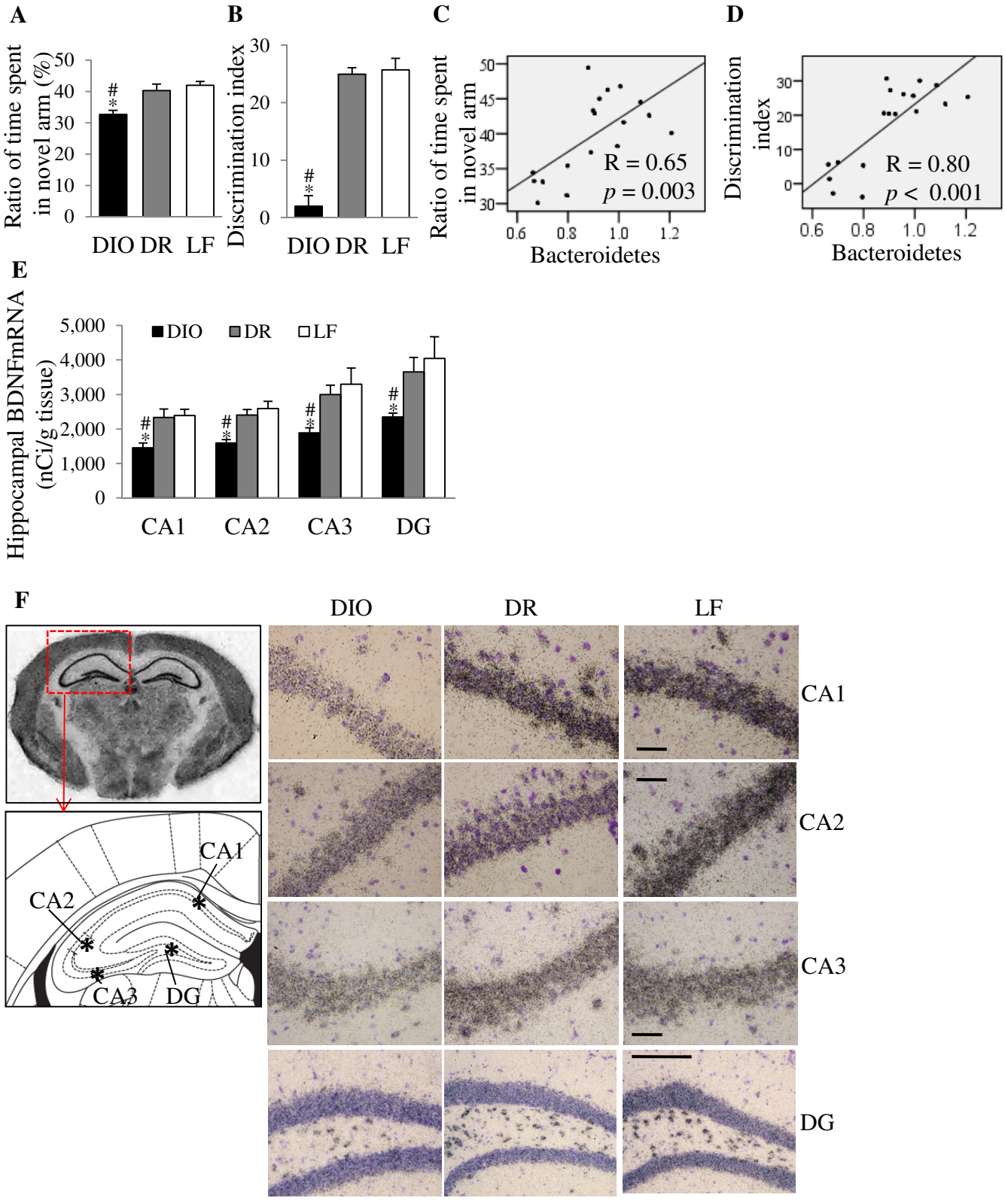
A
Ratio of time spent in novel arm (%)
50
40
30
20
10
0
#
*
DIO DR LF
B
Discrimination index
30
20
10
0
#
*
DIO DR LF
C
Ratio of time spent in novel arm
50
45
40
35
30
R = 0.65
p = 0.003
0.6 0.8 1.0 1.2
Bacteroidetes
D
Discrimination index
30
20
10
0
R = 0.80
p < 0.001
0.6 0.8 1.0 1.2
Bacteroidetes
E
Hippocampal BDNFmRNA (nCi/g tissue)
5,000
4,000
3,000
2,000
1,000
0
DIO
DR
LF
CA1 CA2 CA3 DG
F
DIO
DR
LF
CA1
CA2
CA3
DG